Published in final edited form as:
Urolithiasis. 2015 January ; 43(0 1): 13–17. doi:10.1007/s00240-014-0702-z.

Micro-CT imaging of Randall's plaques

James C. Williams Jr,
Department of Anatomy and Cell Biology, Indiana University School of Medicine, 635 Barnhill Drive MS 5055Y, Indianapolis, IN 46202-5120, USA

James E. Lingeman,
International Kidney Stone Institute, Methodist Hospital, Indianapolis, IN, USA

Fredric L. Coe,
Nephrology Section, University of Chicago, Chicago, IL, USA

Elaine M. Worcester, and
Nephrology Section, University of Chicago, Chicago, IL, USA

Andrew P. Evan
Department of Anatomy and Cell Biology, Indiana University School of Medicine, 635 Barnhill Drive MS 5055Y, Indianapolis, IN 46202-5120, USA

International Kidney Stone Institute, Methodist Hospital, Indianapolis, IN, USA

James C. Williams: jwillia3@iupui.edu

Abstract

Micro-computed tomographic imaging (micro-CT) provides unprecedented information on stone structure and mineral composition. High-resolution micro-CT even allows visualization of the lumens of tubule and/or vessels within Randall's plaque, on stones or in papillary biopsies, thus giving a non-destructive way to study these sites of stone adhesion. This paper also shows an example of a stone growing on a different anchoring mechanism: a mineral plug within the lumen of a Bellini duct (BD plug). Micro-CT shows striking structural differences between stones that have grown on Randall's plaque and those that have grown on BD plugs. Thus, Randall's plaque can be distinguished by micro-CT, and this non-destructive method shows great promise in helping to elucidate the different mechanisms by which small stones are retained in the kidney during the development of nephrolithiasis.

Keywords

Nephrolithiasis; Imaging; Kidney stones; Computed tomography

Correspondence to: James C. Williams, Jr, jwillia3@iupui.edu.

Conflict of interest T he authors declare that they have no conflict of interest.

Ethical standard All studies on humans were approved by the appropriate ethics committee and were performed in accordance with the ethical standards laid down in the 1964 Declaration of Helsinki and its later amendments. All persons gave their informed consent prior to their inclusion in the studies.

Introduction

Micro-computed tomographic imaging (micro-CT) is a technique developed in the 1980s but first applied to urinary stones around the year 2000 [1]. Micro-CT utilizes multiple X-ray images of a specimen to reconstruct the three-dimensional structure as visible by differences in X-ray attenuation [2]. Urinary stones are composed of minerals that vary in their effective atomic number [3], and so micro-CT provides an excellent way to visualize stone structure in vitro [2].

Randall's plaques contain apatite [4], which has the highest effective atomic number of all the common stone minerals [3]. Thus, even when the apatite crystals are rather diffusely distributed in tissue, they can be visualized by X-rays in high contrast with surrounding tissue [5]. In this way, the three-dimensional arrangement of these tissue calcifications can be studied.

But Randall's plaques are also known to be visible on stones [6, 7], even stones that have been passed spontaneously. For example, Cifuentes et al. examined 500 stones that had been passed by stone formers and delivered for analysis, and found 142 of these with a concave surface, and 61 of these bore remnants of what appeared to be Randall's plaque [8]. This identity was confirmed by identifying the presence of calcified renal tubules within the apatite remnant on several similar stones [9].

We have found that micro-CT allows the visualization of Randall's plaques in tissue and stones removed from patients with various forms of calcium oxalate stone disease, and this paper details the morphologic differences of Randall's plaque and duct of Bellini (BD) plugs.

Methods

Stones and papillary biopsies were obtained from consenting patients being treated for kidney stones, as previously described [4]. Micro-CT was performed on specimens, in vitro, using a Skyscan 1172 system (Bruker-MicroCT, Kontich, Belgium). Typical scans utilized 50 kV with a 0.5 mm Al filter, rotating the specimen 0.4° for each X-ray image. Reconstruction voxel size ranged 0.9–5.6 μm for images shown. Viewing of reconstructed image stacks was accomplished using ImageJ (www.imagej.nih.gov) and Vaa3D (www.vaa3d.org).

Recent characterization of Randall's plaque has been done in idiopathic calcium oxalate stone formers, a specific form of stone disease in which the patients show no systemic disorder other than familial (idiopathic) hypercalciuria [10]. These stone formers appear to initiate all of their stones on interstitial Randall's plaque [11, 12], and it is from this kind of stone former that the Randall's plaque examples in this paper are taken. Randall's plaque has also been seen in other types of stone formers [13], but the importance of interstitial plaque to initiation of stones in those other groups has not been studied.

To illustrate the nature of Randall's plaque, and its distinction from other mechanisms by which stones may be retained within the kidney during the earliest stages of growth [14], we

also show a stone taken from a patient in which apatite was deposited from the urine onto the end of a BD plug also formed from apatite.

Imaging Randall's plaque in tissue

Figure 1 shows an example of a biopsy from the papilla of a calcium oxalate stone former having dense Randall's plaque visible at the papillary surface. The micro-CT reconstruction of the densest portion of the mineralized regions in this biopsy reveals several features that we regularly see with Randall's plaque: first, the interstitial mineralization shows no layering in the accumulation of apatite that occurs (which is quite unlike what has been seen in apatite stones [15], as described below). It would seem that an entire region of interstitial connective tissue becomes mineralized, with the density of apatite reaching some maximum value that remains uniform with the densest portions of Randall's plaque. Second, this interstitial mineralization consistently shows cylindrical void regions that have diameters consistent with their representing lumens of tubules and vessels in the papilla. Third, the periphery of the dense region gives way to less dense mineralization of interstitium, where it is often possible to visualize individual tubules that are mineralized, with the surrounding interstitium relatively devoid of mineral.

Previous work has demonstrated that Randall's plaque consists of interstitial mineralization that begins around the thin limbs of Henle's loop [10]. The micro-CT images typically show tubules surrounded by mineral at the edges of Randall's plaque, and the diameter of these tubular segments is consistent with their being thin limbs. For example, a tubule surrounded by mineral at the edge of the field shown in the inset in Fig. 1b has a lumen of size 21 μm at its narrowest portion and 27 μm at its widest. This size is consistent with the tubule being a thin limb.

Note that the form of interstitial mineralization that is seen in classic Randall's plaque differs dramatically from the accumulation of mineral in tubular lumens, as seen in at least eight other forms of stone diseases [13]. In Randall's plaque, the mineral is initially deposited within the basement membrane of thin limbs of Henle's loop [10], and in dense forms of the plaque; by histologic staining, it completely fills the interstitium [4]. However, even in the dense forms of Randall's plaque, the tubule lumens are clear of mineral and the epithelium of tubules is normal [4, 13]. In contrast, deposits of mineral in tubule lumens lead to destruction of the epithelial cells and often to gross dilation of the lumen size [13, 16].

As mentioned above, micro-CT images of Randalls plaque show that the apatite mineral can be rather evenly distributed (at least at the micron-size level) through the interstitial space (Fig. 1). This appearance is in contrast to the typical appearance of apatite in urinary stones, in which the apatite mineral appears in layers of alternating high and low density (layers ranging from about 100 to >1,000 μm in thickness) [15]. That is, the deposit of apatite during stone growth in urine often consists of deposition of organic matrix relatively poor in apatite crystals, alternating with dense deposition of apatite crystals with apparently much less matrix. In contrast, the deposition of apatite within the papillary interstitium of the densest regions of Randall's plaque shows relatively even deposition of mineral throughout the interstitial matrix (Fig. 1).

Imaging Randall's plaque on stones

Figure 2 shows micro-CT images of a small calcium oxalate stone that was plucked from a Randall's plaque-bearing papilla during ureteroscopy. The morphology of the Randall's plaque that pulled away with this stone is representative of many such stones that have been examined by micro-CT over the past few years.

The urinary stone in Fig. 2 consists of a head composed mostly of calcium oxalate monohydrate approximately 400 μm tall and 750 μm in diameter. The region of Randall's plaque beneath the stone has a brighter appearance, consistent with it being composed of apatite, and it also contains cylindrical spaces that appear to be lumens of vessels and tubules (Fig. 2). We did not report these structures in our first micro-CT descriptions of Randall's plaque [11], because the scans of those stones were not at a high enough resolution to reveal the luminal spaces. Most of the luminal spaces we have observed by micro-CT in Randall's plaque are 10–20 μm in diameter, making them likely candidates for lumens of thin limbs and capillaries (Figs. 2, 4). Our earliest stone scans were done with a system that allowed, at best, a voxel size of 20 μm and a resolution even poorer than that [11]. Thus, it would not have been possible to have seen the lumens of vessels or thin limbs in those scans. When we have rescanned some of those older patient stones using higher resolution, we do indeed see luminal spaces within the apatite regions we had previously identified as being portions of interstitial Randall's plaque adherent to the stone.

Comparison with non-Randall's plaque stone

Figure 3 shows micro-CT images of a stone that was attached to the renal papilla, but in a patient with many dilated ducts and BD plugs visible during the surgical procedure. The stone consists of a head composed of apatite in the layered morphology commonly seen in apatite stones, which apparently grew onto the end of an apatite plug that occupied a grossly dilated duct of Bellini.

BD plugs of apatite have been recently described in patients forming calcium phosphate stones [17], and the BD plug shown in Fig. 3 has characteristics similar to that reported in that paper: the apatite in the BD plug is densely packed, yielding a high value for X-ray attenuation (the highest value seen for any stone mineral [18]). This apatite also shows signs of having been laid down in incremental layers; note the alternating layers of light and dark within the apatite plug, as shown in Fig. 4. The exterior surface of the apatite plug has well-defined edges high in mineral content, in contrast to Randall's plaque, in which the mineralization of the interstitium declines gradually at its peripheral boundary. The ductal plug shows no cylindrical passage-ways through its structure, which is consistent with its origin being entirely within the lumen of a collecting duct; in contrast, in Randall's plaque the lumens of tubules and vessels can be seen to remain intact through the mineralized interstitium. Finally, the dimensions of the BD plug—in Fig. 3 about 2 mm in diameter and 2.5 mm long—are consistent with the size of a dilated collecting duct. Such dilated ducts, filled with mineral, have been described in a number of forms of stone disease [13].

Figure 4 shows Randall's plaque and BD plug side-by-side, and lists characteristics for each, as just described. Note that the planes of section shown in Fig. 4 are different from those

shown in Figs. 2 and 3. Figure 4 shows sections across the plaque and plug approximately parallel to the original papillary surface. That is, these are cross-sections through the anchoring apatite structure in both cases. Note additionally that the level of magnification is quite different between the plaque and plug; however, even when imaged at higher power the apatite plug shows no evidence of the luminal structures visible in the Randall's plaque.

Summary

By micro-CT, interstitial Randall's plaque is characterized by a relatively even distribution of apatite within the interstitium of the dense portion of the plaque, with apatite density declining gradually at the periphery of the plaque. This is in marked contrast with the alternating layers of high and low X-ray attenuations that characterize a typical apatite stone formed in the urine. Randall's plaque additionally shows the presence of low-attenuation regions of cylindrical shape, which are evidently the luminal spaces of tubules and vascular elements that ran through the calcified interstitium. These characteristics of even mineral distribution within the interstitium and cylindrical voids showing the lumens of tubules and vessels are seen both in the remnants of Randall's plaque adherent to stones and in Randall's plaque visualized within papillary biopsies. These characteristics are quite different from the appearance of apatite in a BD plug. Thus, Randall's plaque can be distinguished by micro-CT, and this non-destructive method shows great promise in helping to elucidate the different mechanisms by which small stones are retained in the kidney during the development of nephrolithiasis.

Acknowledgment

T his work was funded by NIH P01 DK5678.

References

1. Cleveland RO, McAteer JA, Müller R. Time-lapse non-destructive assessment of shock wave damage to kidney stones in vitro using micro-computed tomography. J Acoust Soc Am. 2001; 110:1733–1736. [PubMed: 11681352]
2. Williams JC Jr, McAteer JA, Evan AP, Lingeman JE. Micro-computed tomography for analysis of urinary calculi. Urol Res. 2010; 38:477–484. [PubMed: 20967434]
3. Qu M, et al. Dual-energy dual-source CT with additional spectral filtration can improve the differentiation of non-uric acid renal stones: an ex vivo phantom study. Am J Roentgenol. 2011; 196:1279–1287. [PubMed: 21606290]
4. Evan AP, et al. Randall's plaque of patients with nephrolithiasis begins in basement membranes of thin loops of Henle. J Clin Invest. 2003; 111:607–616. [PubMed: 12618515]
5. Evan AP, et al. Mechanism of formation of human calcium oxalate renal stones on Randall's plaque. Anat Rec. 2007; 290:1315–1323.
6. Randall A. The origin and growth of renal calculi. Ann Surg. 1937; 105:1009–1027. [PubMed: 17856988]
7. Prien EL, Prien EL. Composition and structure of urinary stone. Am J Med. 1968; 45:654–672. [PubMed: 4301160]
8. Cifuentes Delatte L, Miñón Cifuentes J, Medina JA. New studies on papillary calculi. J Urol. 1987; 137:1024–1029. [PubMed: 3573168]
9. Cifuentes Delatte L, Miñón-Cifuentes JL, Medina JA. Papillary stones: calcified renal tubules in Randall's plaques. J Urol. 1985; 133:490–494. [PubMed: 3974005]

10. Evan AP, Lingeman J, Coe FL, Worcester E. Randall's plaque: pathogenesis and role in calcium oxalate nephrolithiasis. Kidney Int. 2006; 69:1313–1318. [PubMed: 16614720]
11. Miller NL, et al. A formal test of the hypothesis that idiopathic calcium oxalate stones grow on Randall's plaque. BJU Int. 2009; 103:966–971. [PubMed: 19021625]
12. Miller NL, et al. In idiopathic calcium oxalate stone-formers, unattached stones show evidence of having originated as attached stones on Randall's plaque. BJU Int. 2010; 105:242–245. [PubMed: 19549258]
13. Coe FL, Evan AP, Lingeman JE, Worcester EM. Plaque and deposits in nine human stone diseases. Urol Res. 2010; 38:239–247. [PubMed: 20625890]
14. Williams JC Jr, McAteer JA. Retention and growth of urinary stones—insights from imaging. J Nephrol. 2013; 26:25–31. [PubMed: 22976521]
15. Pramanik R, Asplin JR, Jackson ME, Williams JC Jr. Protein content of human apatite and brushite kidney stones: significant correlation with morphologic measures. Urol Res. 2008; 36:251–258. [PubMed: 18779958]
16. Evan AP, et al. Apatite deposits in collecting duct lumens produce epithelial cell injury and interstitial inflammation in patients forming brushite renal stones. J Urol. 2004; 171:299.
17. Evan AP, et al. Contrasting histopathology and crystal deposits in kidneys of idiopathic stone formers who produce hydroxyapatite, brushite, or calcium oxalate stones. Anat Rec. 2014; 297:731–748.
18. Zarse CA, et al. Nondestructive analysis of urinary calculi using micro computed tomography. BMC Urol. 2004; 4:15. [PubMed: 15596006]

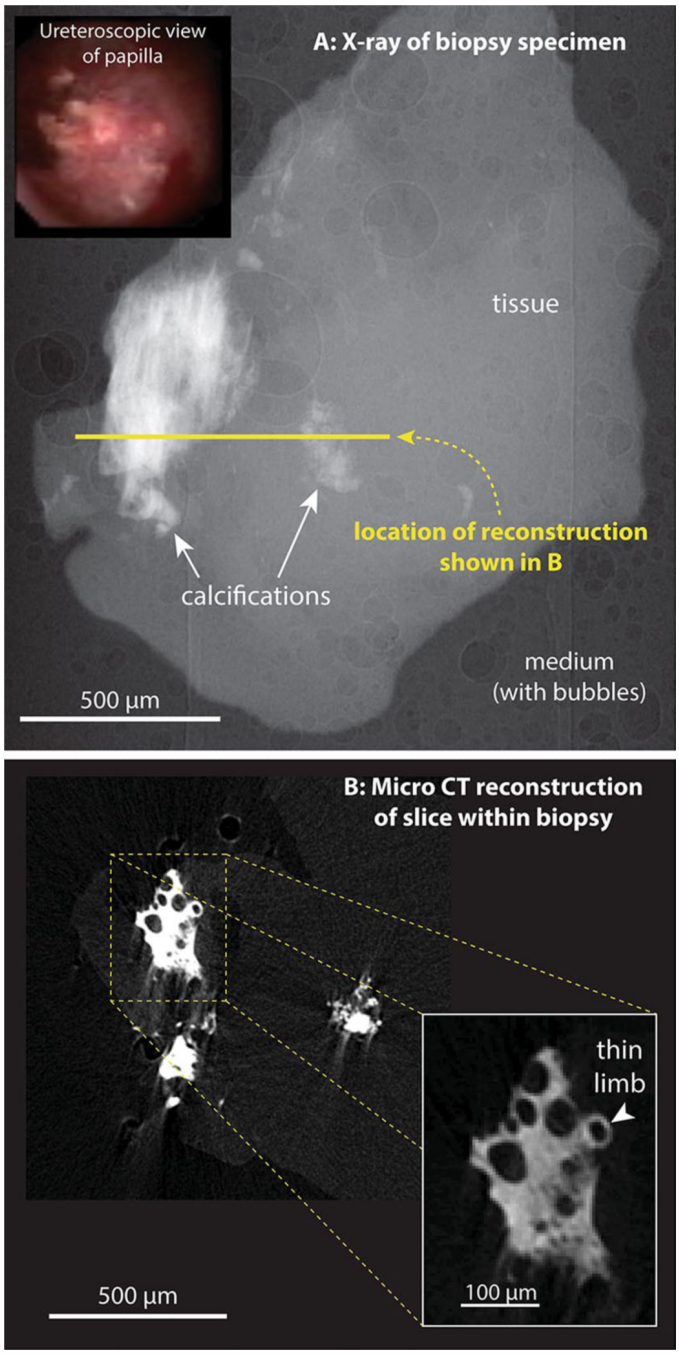

Fig. 1.

Micro-CT imaging of Randall's plaque in human papillary biopsy. **a** Inset ureteroscopic image of papillary surface before biopsy. **a** X-ray image of biopsy. About 450 such images were taken, with the specimen rotated 0.4° between each image. This image series was used for tomographic reconstruction. **b** Reconstructed slice through the biopsy, with inset showing higher magnification of a small portion of Randall's plaque within the tissue

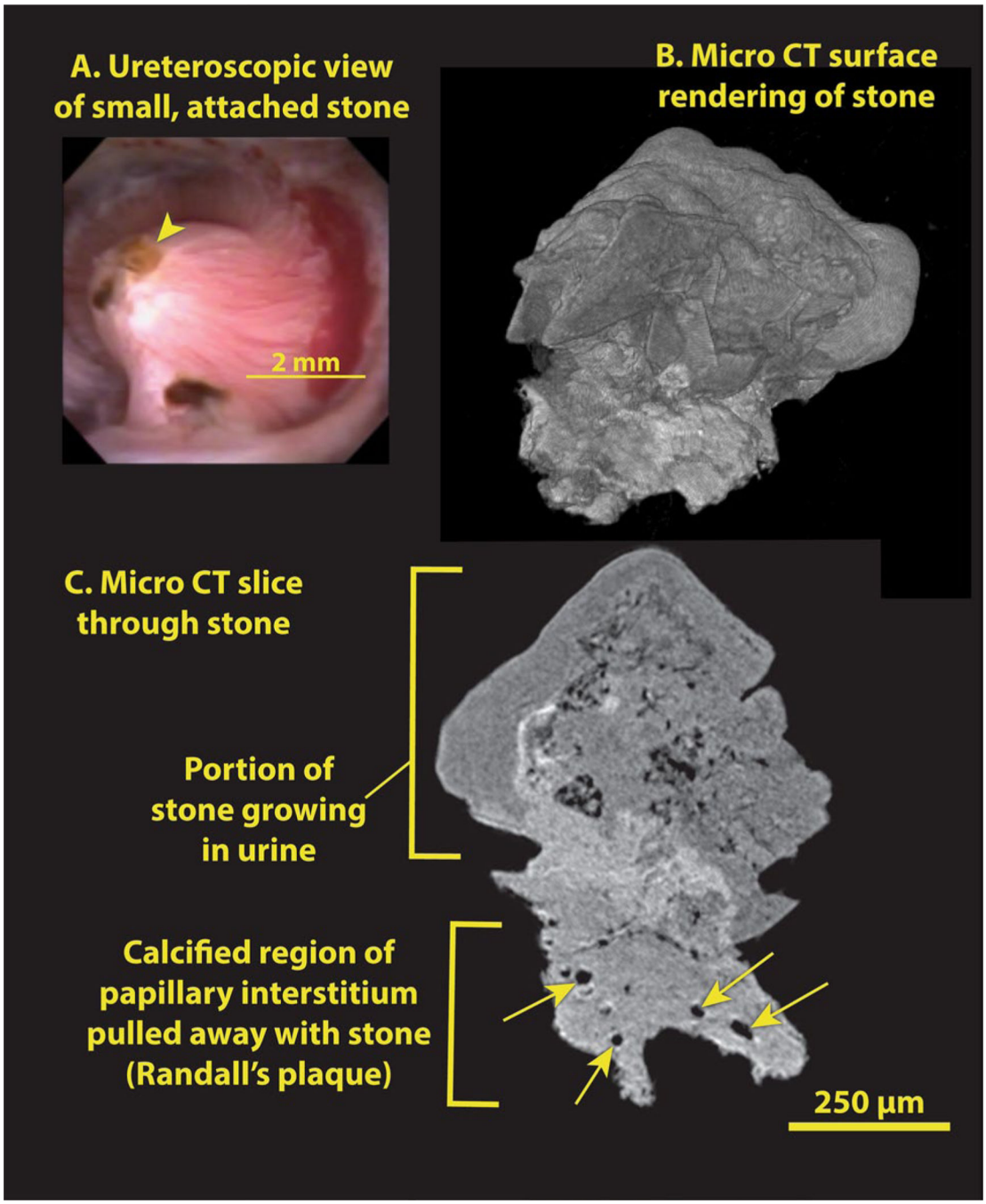

Fig. 2.

Small calcium oxalate monohydrate stone, growing on Randall's plaque. **a** Ureteroscopic view of stone (*arrowhead*) before removal. **b** Surface rendering of the 3D micro-CT image stack shows a relatively smooth stone surface (*top*) with some polyhedral calcium oxalate dihydrate (COD) crystals, but a ragged surface for the Randall's plaque, which was pulled off the papilla tip. **c** Micro-CT image slice showing stone attached to plaque. Some lumens of tubules and/or vessels within the plaque are marked with *arrows*

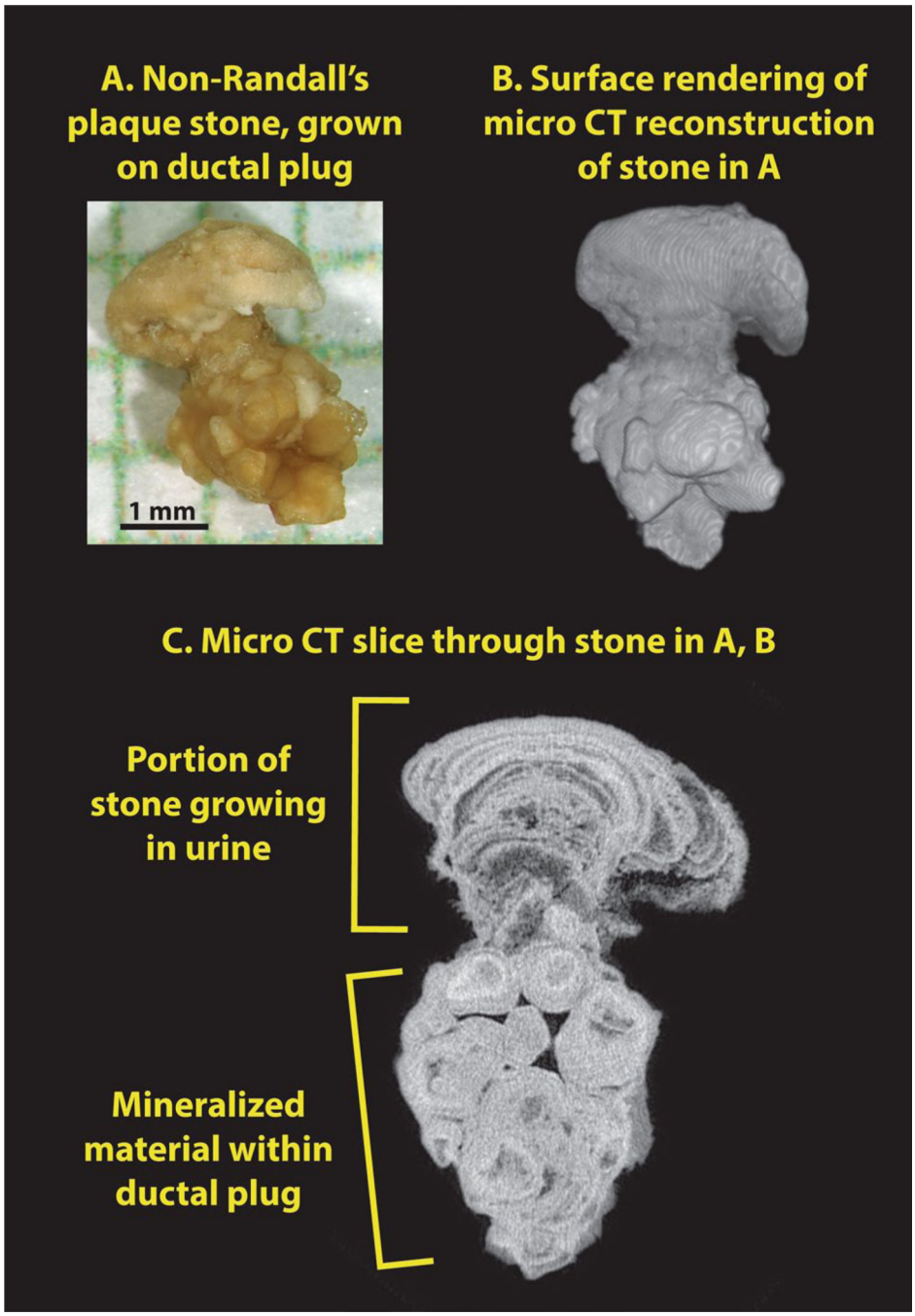

Fig. 3.

Apatite stone growing on end of BD plug. **a** Photograph of stone, after removal, shown on mm-grid paper. **b** Surface reconstruction of stone, showing head of stone on top of apatite plug. **c** Micro-CT image slice, showing the distinct morphologies of the apatite portion that grew in the calyceal urine and the apatite that formed within the BD lumen

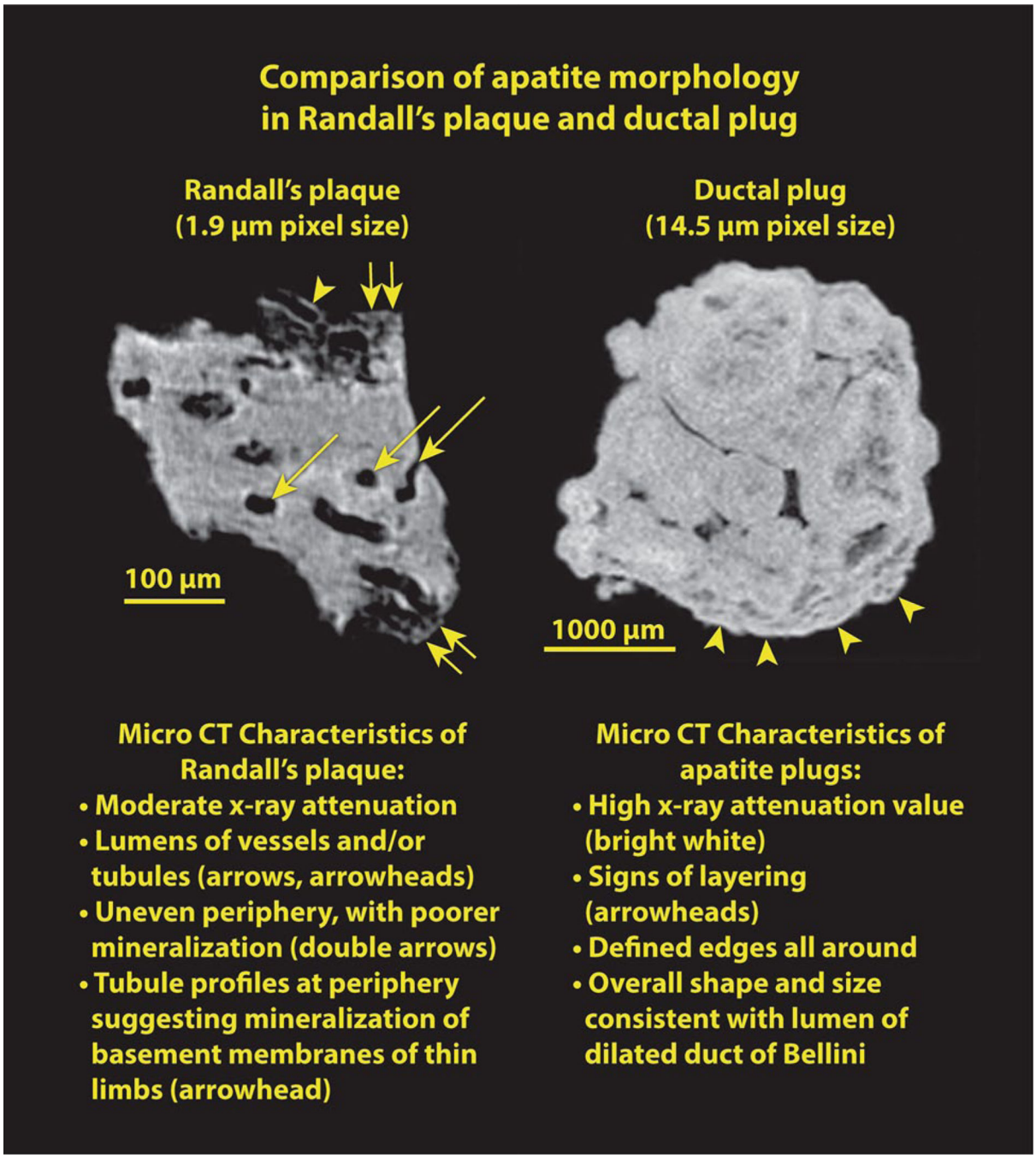

Fig. 4.
Randall's plaque and BD plug, both composed of apatite, shown side by side. See text for details